

Shell-Shaped Quantum Droplet in a Three-Component Ultracold Bose Gas

Yinfeng Ma^{1,2} and Xiaoling Cui^{1,*}

¹*Beijing National Laboratory for Condensed Matter Physics,*

Institute of Physics, Chinese Academy of Sciences, Beijing 100190, China

²*Department of Basic Courses, Naval University of Engineering, Wuhan 430033, China*



(Received 8 January 2024; revised 13 December 2024; accepted 9 January 2025; published 28 January 2025)

Shell-shaped Bose-Einstein condensate is a typical quantum system in curved geometry. Here, we propose a new type of shell-shaped Bose-Einstein condensate with a self-bound character, thereby liberating it from stringent conditions such as microgravity or a fine-tuned trap. Specifically, we consider a three-component (1, 2, 3) ultracold Bose gas where (1, 2) and (2, 3) both form quantum droplets. The two droplets are mutually immiscible due to strong 1–3 repulsion, while still linked by component-2 to form a globally self-bound object. The outer droplet then naturally develops a shell structure without any trapping potential. It is shown that the shell structure can significantly modify the equilibrium density of the core, and lead to unique collective excitations highlighting the core-shell correlation. All results have been demonstrated in a realistic ^{23}Na - ^{39}K - ^{41}K mixture. By extending quantum droplets from flat to curved geometries, this Letter paves the way for future explorations of the interplay of quantum fluctuations and nontrivial real-space topologies in ultracold gases.

DOI: [10.1103/PhysRevLett.134.043402](https://doi.org/10.1103/PhysRevLett.134.043402)

Quantum systems in curved geometries exhibit many distinctive features due to their nontrivial real-space topologies. For instance, a periodic boundary allows a persistent superflow of toroidal Bose-Einstein condensates (BECs) [1,2], and a local curvature gives rise to new topological defects [3–5], interesting few-body physics [6,7], and even non-Hermitian phenomena [8]. As an outstanding case with nontrivial real-space topology, the shell-shaped BEC has attracted a great amount of attention in the field of ultracold atoms [9], and various fascinating properties have been revealed in terms of ground states and thermodynamics [10–13], collective modes [14–16], expansion dynamics [17], and vortex formation [18,19]. These studies are closely related to the experimental efforts in creating shell-shaped BECs, or atomic bubbles, using the shell-shaped potentials under radio-frequency dressing [20,21]. However, the Earth’s gravity prevents the formation of a closed shell in such a setup [22], and consequently a microgravity environment is required. Indeed, the first shell-shaped BEC was recently realized in NASA’s Cold Atom Laboratory aboard the International Space Station [23]. Shortly after that, it was proposed alternatively that binary bosons in an immiscible regime [24,25] can also achieve the shell structure [26]. This idea has been successfully implemented in a recent experiment in the presence of Earth’s gravity [27], where a magic-wavelength optical trap was applied to avoid different gravitational sags between two species.

In this Letter, we introduce a new type of shell-shaped BEC without resorting to any trapping potential, and therefore it does not rely on a microgravity environment or fine-tuned traps as in previous experiments [23,27]. Our scheme is motivated by the recent development of quantum droplet in ultracold atoms, which has been realized in both dipolar gases [28–34] and boson mixtures [35–40]. These droplets are stabilized by a mean-field attraction and the Lee-Huang-Yang repulsion from quantum fluctuations [41], and thus can be self-bound in vacuum. Here, we remark that the self-bound nature of quantum droplets offers an ideal opportunity for creating perfect shell geometry on Earth. This is because in the absence of any external trap, different species in the droplet will fall freely with the same speed and therefore no relative displacement will be produced due to the gravity.

Our scheme of creating a shell-shaped BEC is illustrated in Fig. 1. Specifically, we consider a three-component (1, 2, 3) boson mixture with contact interactions. Here, (1, 2) and (2, 3) both form quantum droplets due to interspecies attractions, while they are immiscible due to strong 1–3 repulsion. The shared component-2 acts as a glue to link two droplets together as a globally self-bound object. In this way, the outer droplet is repelled by the inner core and naturally develops a shell structure in free space. Using a realistic mixture of ^{23}Na - ^{39}K - ^{41}K near $B \sim 150$ G, we show that the outer shell can be efficiently expanded to a larger radius with a thinner width by increasing the core size. To balance with the outer shell, the core droplet exhibits very different equilibrium densities from the vacuum case (without shell). The core-shell correlation can also be

*Contact author: xlcul@iphy.ac.cn

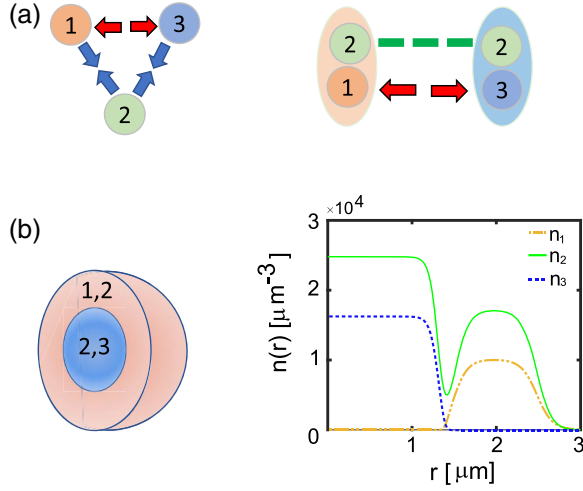


FIG. 1. (a) Interaction model for realizing shell-shaped geometry in three-component (1, 2, 3) bosons. Here, (1, 2) and (2, 3) both form quantum droplets due to interspecies attraction, while the two droplets are immiscible due to 1-3 repulsion. The outer droplet is then shell-shaped. The common component-2 links the whole system together as a self-bound object. (b) Typical half-sphere distribution and associated density profile along the radius direction. Here, we consider a realistic ^{23}Na - ^{39}K - ^{41}K (1-2-3) mixture near $B \sim 150$ G with $a_{23} = -70 a_0$ and $(N_1, N_2, N_3)/10^5 = (5, 10.7, 1.5)$.

manifested in the unique collective excitations of the system. As the first study of quantum droplets in curved geometry, our Letter opens a new avenue for exploring the interplay of quantum fluctuations and nontrivial real-space topologies in the platform of ultracold atoms.

We write the Hamiltonian of three-component boson mixtures $H = \int d\mathbf{r} H(\mathbf{r})$, with $(\hbar = 1)$, as

$$H(\mathbf{r}) = \sum_{i=1}^3 \phi_i^\dagger(\mathbf{r}) \left(-\frac{\nabla^2}{2m_i} \right) \phi_i(\mathbf{r}) + \sum_{ij} \frac{g_{ij}}{2} \phi_i^\dagger \phi_j^\dagger \phi_j \phi_i(\mathbf{r}). \quad (1)$$

Here, \mathbf{r} is the coordinate; m_i and ϕ_i are the mass and field operator of boson species i , respectively; and $g_{ij} = 2\pi a_{ij}/m_{ij}$ is the coupling constant between species i and j , with scattering length a_{ij} and reduced mass $m_{ij} = m_i m_j / (m_i + m_j)$.

For a homogeneous dilute gas with densities $\{n_i\}$ ($i = 1, 2, 3$), the total energy density is composed by the mean-field part $\epsilon_{\text{mf}} = \frac{1}{2} \sum_{ij} g_{ij} n_i n_j$ and a correction from quantum fluctuations,

$$\epsilon_{\text{qf}} = \int \frac{d^3 \mathbf{k}}{2(2\pi)^3} \left[\sum_i (E_{i\mathbf{k}} - \epsilon_{i\mathbf{k}} - g_{ii} n_i) + \sum_{ij} \frac{2m_{ij} g_{ij}^2 n_i n_j}{\mathbf{k}^2} \right], \quad (2)$$

with $\epsilon_{i\mathbf{k}} = k^2/2m_i$, and $E_{i\mathbf{k}}$ the i th Bogoliubov mode [42]. For a general system with inhomogeneous densities, we employ an extended Gross-Pitaevskii (GP) equation incorporating quantum fluctuations,

$$i\partial_t \phi_i = \left(-\frac{\nabla^2}{2m_i} + \sum_j g_{ij} n_j + \frac{\partial \epsilon_{\text{qf}}}{\partial n_i} \right) \phi_i. \quad (3)$$

The ground state can be obtained by the imaginary time evolution of the above coupled equations.

Differing from the miscible three-component droplet in Ref. [42], in this Letter we focus on a qualitatively different situation where components 1 and 3 are immiscible with strong repulsion, while (1, 2) and (2, 3) themselves still form binary droplets; see Fig. 1(a). To achieve this in practice, we consider the boson mixture ^{23}Na - ^{39}K - ^{41}K all at hyperfine state $|F = 1, m_F = -1\rangle$ (denoted as 1-2-3). Near $B \sim 150$ G, we have $(a_{11}, a_{22}, a_{33}, a_{12}, a_{13}) = (52, 30, 63, -50, 213)a_0$ (a_0 is the Bohr radius) [43–45], and a_{23} is highly tunable via a Feshbach resonance at $B_0 = 149.8$ G with width $\Delta B \sim 25$ mG [46]. One can easily check that the required mean-field instabilities, i.e., collapse for 1-2 and 2-3 and phase separation for 1-3, will occur as long as a_{23} is sufficiently attractive.

Our numerical simulations based on (3) indeed produce two mutually immiscible droplets, (1, 2) and (2, 3), as the ground state for above system; see typical density distribution in Fig. 1(b). Remarkably, the whole system is still self-bound due to the presence of component-2. In such an immiscible phase, in principle each droplet can either stay inside as a core or outside as a shell. For the parameter regime we consider, however, the ground state is unique with a higher (lower) density of 2 inside (outside), i.e., $n_2^{\text{core}} > n_2^{\text{shell}}$. This can be attributed to the minimized surface energy under such configuration. For the parameter of a_{23} chosen in this Letter, the core and shell droplets are, respectively, (2, 3) and (1, 2).

We note that similar phenomena of immiscible droplets were also found previously in Helium mixtures [47,48], where a ^4He droplet was coated with a normal ^3He liquid, and in dipole-dipole mixtures with anisotropic density profiles [49,50]. In these studies, a long-range attraction between two droplets is required for their self-binding. In contrast, the binding of immiscible droplets in our case does not rely on any long-range force.

Now we explore the equilibrium expansion of shell droplet by increasing the core size. Let us start with a small core and a thick shell; see Fig. 2(a1), where both droplets display flat-top densities. While increasing the size (or atom number) of the core, the shell is repelled to a larger radius and becomes gradually thinner; see Figs. 2(a2) and 2(a3); meanwhile, its flat-top profile gradually disappears and gives way to a Gaussian distribution with a quite narrow width and low density. In Fig. 2(b), we further extract the maximal density of each component during this process.

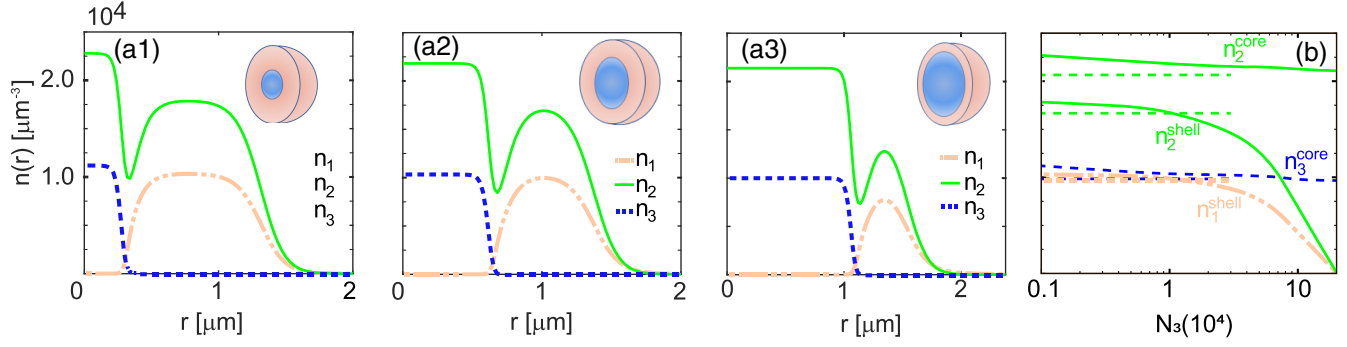


FIG. 2. Expansion of shell (1, 2) droplet while increasing the size of core (2, 3) droplet. Here, we consider the ^{23}Na - ^{39}K - ^{41}K (1-2-3) mixture at $a_{23} = -200a_0$. (a1)–(a3) Density profiles of ground states for different atom numbers $(N_1, N_2, N_3)/10^5 = (1, 1.73, 0.01)$ (a1), $(1, 1.86, 0.1)$ (a2), and $(1, 2.42, 0.5)$ (a3). (b) Maximal densities of the core ($n_2^{\text{core}}, n_3^{\text{core}}$) and shell ($n_1^{\text{shell}}, n_2^{\text{shell}}$) as functions of N_3 . The dashed horizontal colored lines denote the equilibrium density for the shell ($n_i^{\text{shell}} = n_i^{(0)}$) and for the core (n_i^{core}).

One can see that the shell densities decrease rapidly as the core size increases, and eventually a very thin and dilute shell is created.

Because of the shared component-2 as a link, the core and shell droplets, although spatially separated, are strongly correlated with each other. This is clearly reflected in the balance condition as derived below. To start with, let us first consider the shell. Since it can transfer atoms or energy to vacuum, its equilibration is similar to an isolated droplet in vacuum [41] and determined by zero pressure and minimized energy,

$$P_{\text{shell}} = 0; \quad \epsilon_{\text{shell}} = \epsilon_{\text{min}}. \quad (4)$$

In the thermodynamic limit, this gives the same equilibrium density $n_i^{\text{shell}} = n_i^{(0)}$ as the vacuum droplet, as well as a locked density ratio $n_i^{\text{shell}}/n_j^{\text{shell}} = n_i^{(0)}/n_j^{(0)} = \sqrt{g_{jj}/g_{ii}}$. However, the condition (4) does not apply to the core, since it can only transfer atoms to the shell but not directly to vacuum. In this case, the core and shell should have the same pressure and chemical potential (of the shared component-2),

$$P_{\text{core}} = 0; \quad \mu_2^{\text{core}} = \mu_2^{\text{shell}}. \quad (5)$$

Two remarks are in order for the second condition in (5). First, it obviously differs from the second condition in (4), and therefore a different equilibrium density can result for the core as compared to the vacuum case. Second, it exactly expresses the correlation between core and shell droplets. Under this condition, the core densities ($\{n_i^{\text{core}}\}$) depend crucially on the shell chemical potential (μ_2^{shell}), and thus can be highly tunable by the shell parameters.

We now analytically derive $\{n_i^{\text{core}}\}$ based on (4), (5). For a thermodynamically large (i, j) droplet with uniform densities $\{n_i, n_j\}$, its total energy density is given by

$$\epsilon = \frac{1}{2}(g_{ii}n_i^2 + g_{jj}n_j^2) + g_{ij}n_in_j + \epsilon_{\text{qf}}. \quad (6)$$

Here, ϵ_{qf} is the correction from quantum fluctuations [41], which determines a dimensionless function $f = \epsilon_{\text{qf}}(15\pi^2/8)m_i^{-3/2}(g_{ii}n_i)^{-5/2}$. Then the chemical potential $\mu_j = \partial\epsilon/\partial n_j$ and pressure $P = \mu_1n_1 + \mu_2n_2 - \epsilon$ can be obtained straightforwardly, and the $P = 0$ condition leads to the equilibrium density

$$n_i = \frac{25\pi}{1024a_{ii}^3} \left(\frac{\frac{1}{2}(g_{jj}c_{ji}^2 + g_{ii}) + g_{ij}c_{ji}}{g_{ii}f} \right)^2, \quad (7)$$

with density ratio $n_j/n_i = c_{ji}$. In this way, μ_j can also be expressed in terms of a single unknown parameter c_{ji} .

For the shell (1, 2) droplet, the second condition in (4) results in a locked density ratio $c_{21}^{\text{shell}} \approx \sqrt{g_{11}/g_{22}}$, and $n_{1,2}^{\text{shell}}$ reproduce $n_{1,2}^{(0)}$ for the vacuum case [41]. Further, μ_2^{shell} can be obtained as a function of c_{21}^{shell} . For the core (2, 3) droplet, by enforcing the second condition in (5), and recalling μ_2^{core} is just parametrized by c_{23}^{core} , we can then solve c_{23}^{core} and further $n_{2,3}^{\text{core}}$ via (7). In Fig. 2(b), $n_{1,2}^{\text{shell}}$ and $n_{2,3}^{\text{core}}$ are respectively shown by horizontal dashed and dotted lines. These analytical predictions fit well to numerical results when the droplets are in thermodynamical limit.

In Figs. 3(a) and 3(b), we further show how the core densities $n_{2,3}^{\text{core}}$ and their ratio c_{23}^{core} vary with a_{23} . One can see that both $n_{2,3}^{\text{core}}$ and c_{23}^{core} change sensitively with a_{23} , and their deviations from the vacuum values ($n_{2,3}^{(0)}$ and $c_{23}^{(0)} \sim \sqrt{g_{33}/g_{22}}$) get more significant if a_{23} gets more attractive. This can be attributed to the larger mismatch of $\mu_2^{(0)}$ for isolated (2, 3) and (1, 2) droplets in vacuum; see the inset of Fig. 3(b). As a result, to balance the two chemical potentials as required by (5), the core has to adjust its densities to change μ_2^{core} , such that it can match $\mu_2^{(0)}$ in the shell. This is how the correlation is built up between core and shell, and the modified core densities are a direct

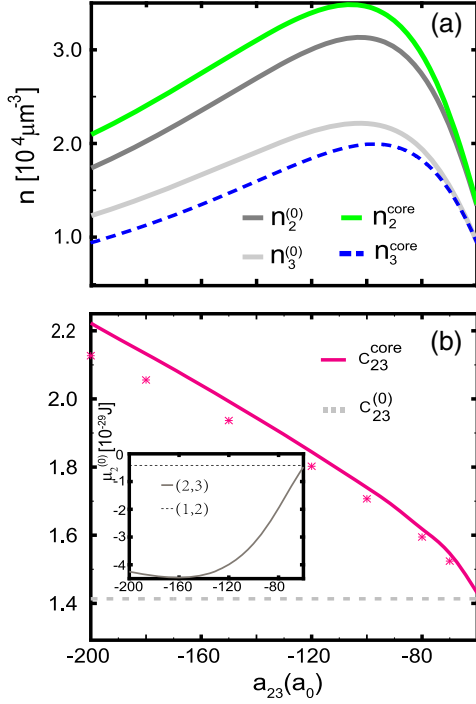


FIG. 3. Tunable equilibrium densities of the core (2, 3) droplet in ^{23}Na - ^{39}K - ^{41}K (1-2-3) mixture. (a) Equilibrium densities $n_{2,3}^{\text{core}}$ as functions of a_{23} , as compared to $n_{2,3}^{(0)}$ in vacuum. (b) Density ratio $c_{23}^{\text{core}} = n_2^{\text{core}}/n_3^{\text{core}}$ and its vacuum counterpart $c_{23}^{(0)} = n_2^{(0)}/n_3^{(0)}$ as functions of a_{23} . The stars (\star) show numerical results by simulating the GP equations (3) in imaginary time for large atom number $N_i = 10^5$ – 10^6 . Inset shows $\mu_2^{(0)}$ for isolated (2, 3) and (1, 2) droplets in vacuum.

evidence of such correlation. In this way, the core-shell structure presents a rare situation where the equilibrium density of a quantum droplet can be efficiently tuned by its surrounding environment.

The core-shell correlation can also lead to unique collective excitations. Here, we assume a small density fluctuation for component- i ,

$$\delta\phi_i = \exp(-i\mu_i t) \sum_j (u_j^{(i)} \exp(-i\omega_j t) + v_j^{(i)*} \exp(i\omega_j t)). \quad (8)$$

By linearizing the GP equation (3) in terms of $\{\delta\phi_i, \delta\phi_i^*\}$, we obtain the equations for collective excitations and further solve the eigenmodes $\{u_{j;l}^{(i)}, v_{j;l}^{(i)}\}$ and eigenenergies $\{\omega_{j;l}\}$ in each angular momentum (l) sector [51]. In Fig. 4(a), we show the four lowest excitations modes with $j = 0$ and $l = 0, 2, 3, 4$, where $l = 0$ corresponds to breathing mode and the rest three are surface modes. Note that the $l = 1$ dipole mode is associated with the center-of-mass motion and is therefore with zero excitation energy for self-bound droplets (see also [41]). Here, we see that

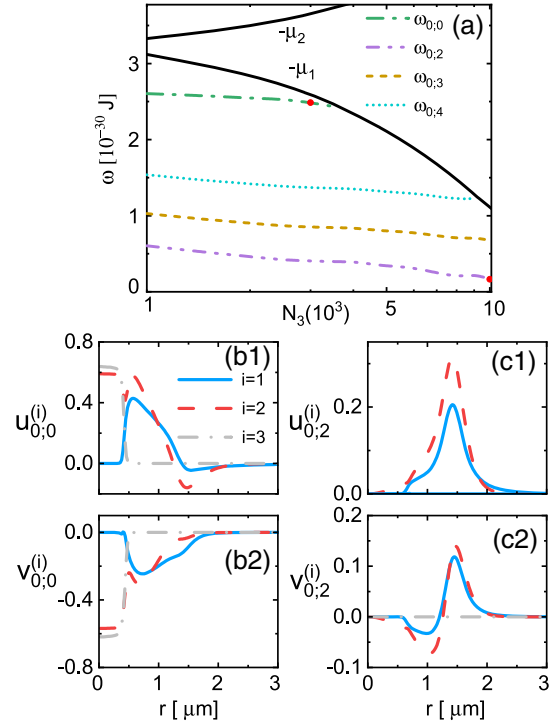


FIG. 4. Collective excitations of ^{23}Na - ^{39}K - ^{41}K (1-2-3) mixture on top of the equilibrium states in Fig. 2(b). In (a), four lowest breathing modes $\omega_{j=0;l=0,2,3,4}$ in different angular momentum channels are shown below the atom emission threshold $\{-\mu_i\}$. (b1),(b2) and (c1),(c2) show the radial excitation modes $\{u_{0;l}^{(i)}(r), v_{0;l}^{(i)}(r)\}$ for, respectively, $l = 0$ breathing mode at $N_3 = 3000$ and $l = 2$ surface mode at $N_3 = 10^4$.

while increasing the core size (N_3), both the breathing and surface modes gradually vanish and merge into the atom emission threshold ($-\mu_1$). This is distinct from the case without shell structure, where all excitation modes become more stable while increasing the droplet size [41]. To clearly see the nature of these modes, we plot out the typical radial wave functions $\{u_{0;l}^{(i)}(r), v_{0;l}^{(i)}(r)\}$ in Figs. 4(b1), 4(b2), 4(c1), and 4(c2), respectively, for $l = 0$ breathing and $l = 2$ surface modes. Remarkably, the breathing mode displays strong core-shell correlations, where all the three components (in both core and shell) oscillate in phase with visible $u^{(i)}$ and $v^{(i)}$. Such correlated excitations can be attributed to the linking effect of shared component. In comparison, the surface modes are mostly localized in the shell but occupy little in the core. In this case, the core and shell are well separated and these excitations are solely tied with the curved geometry. As the core gets larger, the thinner shell becomes less bound and finally it cannot stabilize the surface excitations, as manifested by the disappearance of surface modes at $\omega_{0;l} = -\mu_1$.

In summary, we have demonstrated a scheme to create shell-shaped quantum droplet in ultracold boson mixtures without resorting to any trapping potential. A number of

unique properties associated with the shell structure have been revealed, including its equilibrium expansion, modified core densities by core-shell balance, as well as the correlated and localized collective excitations. We have utilized a ^{23}Na - ^{39}K - ^{41}K mixture to demonstrate these results, while other atomic candidates may also be possible given a growing number of bosonic mixtures now available with tunable interactions [45,46,52–55]. In fact, quantum mixtures of three different atomic species have been successfully realized in ultracold experiments [56,57]. Moreover, to facilitate the detection of shell-shaped droplets, we suggest preparing the core-shell structure initially in an isotropic harmonic trap, with optimized mode matching to the ground state droplet [40]. In this way the system is expected to quickly relax to the shell-shaped droplet after releasing from the trap. The $l = 0$ breathing mode can be naturally produced during the releasing process [58,59], while the $l > 0$ surface mode can be excited via certain anisotropic distortion of the cloud [60,61]. The time periods of these modes crucially rely on the interaction strength, and in general a more tightly bound droplet (more attractive a_{ij}) will lead to a more rapid collective oscillation [41,51].

Our Letter opens up a new avenue to study quantum droplets with nontrivial real-space topologies, which can drive many intriguing phenomena due to the interplay with quantum fluctuations. One interesting subject would be the dynamical property of shell droplets, such as vortex formation and quench dynamics. Given the unique properties of self-bound droplets in vortices [62–67] and dynamics [58,59,68–71], one can imagine dramatic consequences in combination with the compactness and local curvature of shell geometry. Moreover, it is worthwhile to study quantum fluctuation effects when the shell becomes thin enough and behaves as effectively 2D [where Eq. (2) is no longer applicable]. Given that a 2D droplet can be supported at arbitrarily low density [72], we can expect a stable shell even at a very large radius with an extremely thin width. Finally, we note that the present scheme can be directly generalized to quasi-2D systems in creating a toroidal droplet. More fascinating physics of these curved droplets remain to be explored in future.

Acknowledgments—We are grateful to Tin-Lun Ho for valuable discussions which motivated this project. The work is supported by the National Natural Science Foundation of China (12074419, 12134015, 12205365, 92476104), and the Strategic Priority Research Program of Chinese Academy of Sciences (XDB33000000).

-
- [1] C. Ryu, M.F. Andersen, P. Cladé, V. Natarajan, K. Helmerson, and W.D. Phillips, Observation of persistent flow of a Bose-Einstein condensate in a toroidal trap, *Phys. Rev. Lett.* **99**, 260401 (2007).
 [2] A. Ramanathan, K.C. Wright, S.R. Muniz, M. Zelan, W.T. Hill, C.J. Lobb, K. Helmerson, W.D. Phillips, and

- G.K. Campbell, Superflow in a toroidal Bose–Einstein condensate: An atom circuit with a tunable weak link, *Phys. Rev. Lett.* **106**, 130401 (2011).
 [3] A.M. Turner, V. Vitelli, and D.R. Nelson, Vortices on curved surfaces, *Rev. Mod. Phys.* **82**, 1301 (2010).
 [4] T.-L. Ho and B. Huang, Spinor condensates on a cylindrical surface in synthetic gauge fields, *Phys. Rev. Lett.* **115**, 155304 (2015).
 [5] X.-F. Zhou, C. Wu, G.-C. Guo, R. Wang, H. Pu, and Z.-W. Zhou, Synthetic Landau levels and spinor vortex matter on a haldane spherical surface with a magnetic monopole, *Phys. Rev. Lett.* **120**, 130402 (2018).
 [6] J. Zhang and T.-L. Ho, Potential scattering on a spherical surface, *J. Phys. B* **51**, 115301 (2018).
 [7] Z.-Y. Shi and H. Zhai, Emergent gauge field for a chiral bound state on curved surface, *J. Phys. B* **50**, 184006 (2017).
 [8] C. Lv, R. Zhang, Z. Zhai, and Q. Zhou, Curving the space by non-Hermiticity, *Nat. Commun.* **13**, 2184 (2022).
 [9] A. Tononi and L. Salasnich, Low-dimensional quantum gases in curved geometries, *Nat. Rev. Phys.* **5**, 398 (2023).
 [10] A. Tononi and L. Salasnich, Bose-Einstein condensation on the surface of a sphere, *Phys. Rev. Lett.* **123**, 160403 (2019).
 [11] S. Prestipino and P.V. Giaquinta, Ground state of weakly repulsive soft-core bosons on a sphere, *Phys. Rev. A* **99**, 063619 (2019).
 [12] B. Rhyno, N. Lundblad, D.C. Aveline, C. Lannert, and S. Vishveshwara, Thermodynamics in expanding shell-shaped Bose-Einstein condensates, *Phys. Rev. A* **104**, 063310 (2021).
 [13] M. Ciardi, F. Cinti, G. Pellicane, and S. Prestipino, Super-solid phases of bosonic particles in a bubble trap, *Phys. Rev. Lett.* **132**, 026001 (2024).
 [14] C. Lannert, T.C. Wei, and S. Vishveshwara, Dynamics of condensate shells: Collective modes and expansion, *Phys. Rev. A* **75**, 013611 (2007).
 [15] K. Padavić, K. Sun, C. Lannert, and S. Vishveshwara, Physics of hollow Bose-Einstein condensates, *Europhys. Lett.* **120**, 20004 (2017).
 [16] K. Sun, K. Padavić, F. Yang, S. Vishveshwara, and C. Lannert, Static and dynamic properties of shell-shaped condensates, *Phys. Rev. A* **98**, 013609 (2018).
 [17] A. Tononi, F. Cinti, and L. Salasnich, Quantum bubbles in microgravity, *Phys. Rev. Lett.* **125**, 010402 (2020).
 [18] K. Padavić, K. Sun, C. Lannert, and S. Vishveshwara, Vortex-antivortex physics in shell-shaped Bose-Einstein condensates, *Phys. Rev. A* **102**, 043305 (2020).
 [19] S.J. Bereta, M.A. Caracanhas, and A.L. Fetter, Superfluid vortex dynamics on a spherical film, *Phys. Rev. A* **103**, 053306 (2021).
 [20] O. Zobay and B.M. Garraway, Two-dimensional atom trapping in field-induced adiabatic potentials, *Phys. Rev. Lett.* **86**, 1195 (2001).
 [21] O. Zobay and B.M. Garraway, Atom trapping and two-dimensional Bose-Einstein condensates in field-induced adiabatic potentials, *Phys. Rev. A* **69**, 023605 (2004).
 [22] Y. Colombe, E. Knyazchyan, O. Morizot, B. Mercier, V. Lorent, and H. Perrin, Ultracold atoms confined in rf-induced two-dimensional trapping potentials, *Europhys. Lett.* **67**, 593 (2004).

- [23] R. A. Carollo, D. C. Aveline, B. Rhyno, S. Vishveshwara, C. Lannert, J. D. Murphree, E. R. Elliott, J. R. Williams, R. J. Thompson, and N. Lundblad, Observation of ultracold atomic bubbles in orbital microgravity, *Nature (London)* **606**, 281 (2022).
- [24] T.-L. Ho and V.B. Shenoy, Binary mixtures of Bose condensates of alkali atoms, *Phys. Rev. Lett.* **77**, 3276 (1996).
- [25] H. Pu and N.P. Bigelow, Properties of two-species Bose condensates, *Phys. Rev. Lett.* **80**, 1130 (1998).
- [26] A. Wolf, P. Boegel, M. Meister, A. Balaž, N. Gaaloul, and M. A. Efremov, Shell-shaped Bose-Einstein condensates based on dual-species mixtures, *Phys. Rev. A* **106**, 013309 (2022).
- [27] F. Jia, Z. Huang, L. Qiu, R. Zhou, Y. Yan, and D. Wang, Expansion dynamics of a shell-shaped Bose-Einstein condensate, *Phys. Rev. Lett.* **129**, 243402 (2022).
- [28] I. Ferrier-Barbut, H. Kadau, M. Schmitt, M. Wenzel, and T. Pfau, Observation of quantum droplets in a strongly dipolar Bose gas, *Phys. Rev. Lett.* **116**, 215301 (2016).
- [29] M. Schmitt, M. Wenzel, F. Böttcher, I. Ferrier-Barbut, and T. Pfau, Self-bound droplets of a dilute magnetic quantum liquid, *Nature (London)* **539**, 259 (2016).
- [30] I. Ferrier-Barbut, M. Schmitt, M. Wenzel, H. Kadau, and T. Pfau, Liquid quantum droplets of ultracold magnetic atoms, *J. Phys. B* **49**, 214004 (2016).
- [31] L. Chomaz, S. Baier, D. Petter, M. J. Mark, F. Wächtler, L. Santos, and F. Ferlaino, Quantum-fluctuation-driven crossover from a dilute Bose-Einstein condensate to a macrodroplet in a dipolar quantum fluid, *Phys. Rev. X* **6**, 041039 (2016).
- [32] L. Tanzi, E. Lucioni, F. Famà, J. Catani, A. Fioretti, C. Gabbanini, R. N. Bisset, L. Santos, and G. Modugno, Observation of a dipolar quantum gas with metastable supersolid properties, *Phys. Rev. Lett.* **122**, 130405 (2019).
- [33] F. Böttcher, J. N. Schmidt, M. Wenzel, J. Hertkorn, M. Guo, T. Langen, and T. Pfau, Transient supersolid properties in an array of dipolar quantum droplets, *Phys. Rev. X* **9**, 011051 (2019).
- [34] L. Chomaz, D. Petter, P. Ilzhöfer, G. Natale, A. Trautmann, C. Politi, G. Durastante, R. M. W. van Bijnen, A. Patscheider, M. Sohmen, M. J. Mark, and F. Ferlaino, Long-lived and transient supersolid behaviors in dipolar quantum gases, *Phys. Rev. X* **9**, 021012 (2019).
- [35] C. R. Cabrera, L. Tanzi, J. Sanz, B. Naylor, P. Thomas, P. Cheiney, and L. Tarruell, Quantum liquid droplets in a mixture of Bose-Einstein condensates, *Science* **359**, 301 (2018).
- [36] P. Cheiney, C. R. Cabrera, J. Sanz, B. Naylor, L. Tanzi, and L. Tarruell, Bright soliton to quantum droplet transition in a mixture of Bose-Einstein condensates, *Phys. Rev. Lett.* **120**, 135301 (2018).
- [37] G. Semeghini, G. Ferioli, L. Masi, C. Mazzinghi, L. Wolswijk, F. Minardi, M. Modugno, G. Modugno, M. Inguscio, and M. Fattori, Self-bound quantum droplets of atomic mixtures in free space, *Phys. Rev. Lett.* **120**, 235301 (2018).
- [38] C. D'Errico, A. Burchianti, M. Prevedelli, L. Salasnich, F. Ancilotto, M. Modugno, F. Minardi, and C. Fort, Observation of quantum droplets in a heteronuclear bosonic mixture, *Phys. Rev. Res.* **1**, 033155 (2019).
- [39] A. Burchianti, C. D'Errico, M. Prevedelli, L. Salasnich, F. Ancilotto, M. Modugno, F. Minardi, and C. Fort, A dual-species Bose-Einstein condensate with attractive interspecies interactions, *Condens. Matter* **5**, 21 (2020).
- [40] Z. Guo, F. Jia, L. Li, Y. Ma, J. M. Hutson, X. Cui, and D. Wang, Lee-Huang-Yang effects in the ultracold mixture of ^{23}Na and ^{87}Rb with attractive interspecies interactions, *Phys. Rev. Res.* **3**, 033247 (2021).
- [41] D. S. Petrov, Quantum mechanical stabilization of a collapsing Bose-Bose mixture, *Phys. Rev. Lett.* **115**, 155302 (2015).
- [42] Y. Ma, C. Peng, and X. Cui, Borromean droplet in three-component ultracold Bose gases, *Phys. Rev. Lett.* **127**, 043002 (2021).
- [43] M. Lysebo and L. Veseth, Feshbach resonances and transition rates for cold homonuclear collisions between ^{39}K and ^{41}K atoms, *Phys. Rev. A* **81**, 032702 (2010).
- [44] A. Viel and A. Simoni, Feshbach resonances and weakly-bound molecular states of boson-boson and boson-fermion NaK pairs, *Phys. Rev. A* **93**, 042701 (2016).
- [45] T. A. Schulze, T. Hartmann, K. K. Voges, M. W. Gempel, E. Tiemann, A. Zenesini, and S. Ospelkaus, Feshbach spectroscopy and dual-species Bose-Einstein condensation of ^{29}Na - ^{39}K mixtures, *Phys. Rev. A* **97**, 023623 (2018).
- [46] L. Tanzi, C. R. Cabrera, J. Sanz, P. Cheiney, M. Tomza, and L. Tarruell, Feshbach resonances in potassium Bose-Bose mixtures, *Phys. Rev. A* **98**, 062712 (2018).
- [47] M. Pi, R. Mayol, and M. Barranco, Structure of large ^3He - ^4He mixed drops around a dopant molecule, *Phys. Rev. Lett.* **82**, 3093 (1999).
- [48] M. Barranco, R. Guardiola, S. Hernández, R. Mayol, J. Navarro, and M. Pi, Helium nanodroplets: An overview, *J. Low Temp. Phys.* **142**, 1 (2006).
- [49] R. N. Bisset, L. A. Ardila, and L. Santos, Quantum droplets of dipolar mixtures, *Phys. Rev. Lett.* **126**, 025301 (2021).
- [50] J. C. Smith, D. Baillie, and P. B. Blakie, Quantum droplet states of a binary magnetic gas, *Phys. Rev. Lett.* **126**, 025302 (2021).
- [51] See Supplemental Material at <http://link.aps.org/supplemental/10.1103/PhysRevLett.134.043402> for more details on the analysis of equilibrium densities and collective modes.
- [52] G. Thalhammer, G. Barontini, L. De Sarlo, J. Catani, F. Minardi, and M. Inguscio, Double species Bose-Einstein condensate with tunable interspecies interactions, *Phys. Rev. Lett.* **100**, 210402 (2008).
- [53] L. Wacker, N. B. Jørgensen, D. Birkmose, R. Horchani, W. Ertmer, C. Klempt, N. Winter, J. Sherson, and J. J. Arlt, Tunable dual-species Bose-Einstein condensates of ^{39}K and ^{87}Rb , *Phys. Rev. A* **92**, 053602 (2015).
- [54] F. Wang, X. Li, D. Xiong, and D. Wang, A double species ^{23}Na and ^{87}Rb Bose-Einstein condensate with tunable miscibility via an interspecies Feshbach resonance, *J. Phys. B: At. Mol. Opt. Phys.* **49**, 015302 (2015).
- [55] M. Grobner, P. Weinmann, E. Kirilov, H.-C. Nagerl, P. S. Julienne, C. Ruth Le Sueur, and J. M. Hutson, Observation of interspecies Feshbach resonances in an ultracold ^{39}K - ^{133}Cs mixture and refinement of interaction potentials, *Phys. Rev. A* **95**, 022715 (2017).

- [56] M. Taglieber, A.-C. Voigt, T. Aoki, T. W. Hansch, and K. Dieckmann, Quantum degenerate two-species Fermi-Fermi mixture coexisting with a Bose-Einstein condensate, *Phys. Rev. Lett.* **100**, 010401 (2008).
- [57] C.-H. Wu, I. Santiago, J. W. Park, P. Ahmadi, and M. W. Zwierlein, Strongly interacting isotopic Bose-Fermi mixture immersed in a Fermi sea, *Phys. Rev. A* **84**, 011601(R) (2011).
- [58] G. Ferioli, G. Semeghini, S. Terradas-Briansó, L. Masi, M. Fattori, and M. Modugno, Dynamical formation of quantum droplets in a 39K mixture, *Phys. Rev. Res.* **2**, 013269 (2020).
- [59] Y. Ma and X. Cui, Quantum-fluctuation-driven dynamics of droplet splashing, recoiling, and deposition in ultracold binary Bose gases, *Phys. Rev. Res.* **5**, 013100 (2023).
- [60] D. S. Jin, J. R. Ensher, M. R. Matthews, C. E. Wieman, and E. A. Cornell, Collective excitations of a Bose-Einstein condensate in a dilute gas, *Phys. Rev. Lett.* **77**, 420 (1996).
- [61] M.-O. Mewes, M. R. Andrews, N. J. van Druten, D. M. Kurn, D. S. Durfee, C. G. Townsend, and W. Ketterle, Collective excitations of a Bose-Einstein condensate in a magnetic trap, *Phys. Rev. Lett.* **77**, 988 (1996).
- [62] Y. Li, Z. Chen, Z. Luo, C. Huang, H. Tan, W. Pang, and B. A. Malomed, Two-dimensional vortex quantum droplets, *Phys. Rev. A* **98**, 063602 (2018).
- [63] X. Zhang, X. Xu, Y. Zheng, Z. Chen, B. Liu, C. Huang, B. A. Malomed, and Y. Li, Semidiscrete quantum droplets and vortices, *Phys. Rev. Lett.* **123**, 133901 (2019).
- [64] M. N. Tengstrand, P. Stürmer, E. Karabulut, and S. M. Reimann, Rotating binary Bose-Einstein condensates and vortex clusters in quantum droplets, *Phys. Rev. Lett.* **123**, 160405 (2019).
- [65] M. Caldara and F. Ancilotto, Vortices in quantum droplets of heteronuclear Bose mixtures, *Phys. Rev. A* **105**, 063328 (2022).
- [66] Q. Gu and X. Cui, Self-bound vortex lattice in a rapidly rotating quantum droplet, *Phys. Rev. A* **108**, 063302 (2023).
- [67] T. A. Yoğurt, U. Tanyeri, A. Keleş, and M. Ö. Oktel, Vortex lattices in strongly confined quantum droplets, *Phys. Rev. A* **108**, 033315 (2023).
- [68] G. E. Astrakharchik and B. A. Malomed, Dynamics of one-dimensional quantum droplets, *Phys. Rev. A* **98**, 013631 (2018).
- [69] G. Ferioli, G. Semeghini, L. Masi, G. Giusti, G. Modugno, M. Inguscio, A. Gallemí, A. Recati, and M. Fattori, Collisions of self-bound quantum droplets, *Phys. Rev. Lett.* **122**, 090401 (2019).
- [70] V. Cikojević, L. Vranješ Markić, M. Pi, M. Barranco, F. Ancilotto, and J. Boronat, Dynamics of equilibration and collisions in ultradilute quantum droplets, *Phys. Rev. Res.* **3**, 043139 (2021).
- [71] C. Fort and M. Modugno, Self-evaporation dynamics of quantum droplets in a ^{41}K - ^{87}Rb mixture, *Appl. Sci.* **11**, 866 (2021).
- [72] D. S. Petrov and G. E. Astrakharchik, Ultradilute low-dimensional liquids, *Phys. Rev. Lett.* **117**, 100401 (2016).